http://dx.doi.org/10.5012/bkcs.2014.35.5.1299

Influence of Electrolyte Composition on Electrochemical Performance of Li-S Cells

Tae Jeong Kim, Bo Ock Jeong, Jeong Yoon Koh, Seok Kim,† and Yongju Jung*

*Department of Chemical Engineering, Korea University of Technology and Education (KOREATECH), Cheonan 330-708, Korea. *E-mail: yjung@koreatech.ac.kr*
†School of Chemical and Biochemical Engineering, Pusan National University, Busan 609-735, Korea
Received November 26, 2013, Accepted January 3, 2014

The electrochemical performance of Li-S cells was investigated in various ternary electrolyte solutions composed of 1,2-dimethoxyethane (DME), tetra(ethylene glycol) dimethyl ether (TGM), and 1,3-dioxolane (DOX). The discharge capacity values and cycle data obtained at each composition were statistically treated with the Minitab program to obtain mixture contour plots, from which the optimal composition of the ternary solvent systems was predicted. The discharge capacities and capacity retention were quite dependent on the electrolyte composition. It was estimated from the contour plots of the capacity at 1.0 C that the discharge capacity sharply increased with a decrease in the TGM content. High capacities greater than 900 mAh/g at 1.0 C were expected for the electrolyte composition with a volume ratio of DME/TGM/DOX = 1/0/1. In contrast, it was predicted from the mixture contour plot of the capacity retention that the cycle performance would significantly increase with an increase in the DME content.

Key Words : Li-S batteries, Ternary electrolyte, DME, TGM, DOX

Introduction

Over the past 15 years, ambient-temperature lithium-sulfur (Li-S) batteries with sulfur-based composite cathodes have been repositioned as the next generation of lithium-based secondary batteries due to their tremendous theoretical capacity (1675 mAh/g-sulfur).[1-4] The redox mechanism of a sulfur cathode is quite different from that of conventional lithium-ion batteries (LIBs). In LIBs, the redox reactions of the cathode (*e.g.*, $LiCoO_2$) and anode (*e.g.*, graphite) are commonly based on the intercalation of lithium ions into the solid host materials. Structural changes do not occur as a result of this intercalation, except for slight changes in lattice parameters. In contrast, the charge (electron) transfer process of a sulfur cathode can be described by interfacial electrochemistry, such as the redox flow cell of a V^{2+}/V^{3+} couple. Redox species such as S_8 and polysulfides (*e.g.*, S_8^{2-}, S_3^{-}, S_3^{2-}) exist in electrolyte solutions and participate in electrode reactions occurring at the electrode/electrolyte interface.[5-8] The dissolution of polysulfides is inevitable and essential to the normal operation of Li-S batteries. For this reason, electrodes (*e.g.*, carbon) with a large surface area and good conductivity are required for the facile redox reactions of S_8/S_8^{2-} and S_3^{-}/S_3^{2-} couples. In addition, it would be very desirable for the enhancement of the cycle life to delicately design the structure of the cathode to confine polysulfides (S_n^{2-} or S_n^{-}) generated during charge/discharge cycles within a specific space, such as a cathode. However, an approach based on using carbon-sulfur composites to provide close electrical contact between sulfur and carbon or on searching for electrolyte systems with low polysulfide solubility would be not effective. In fact, in the late 1990s, the PolyPlus battery company presented a breakthrough for high-capacity Li-S cells operating at ambient temperature with glyme-based electrolytes, which exhibit excellent levels of solubility for polysulfides.[9] This breakthrough triggered many researchers and manufacturers to participate in the development of Li-S batteries. In the early 2000s, Samsung SDI attempted to develop high-capacity Li-S batteries for mobile IT devices through collaboration with the PolyPlus battery company but failed to commercialize the batteries due to the poor cycle properties of sulfur cathodes and lithium anodes. In general, the physicochemical properties of polysulfides, such as their electrochemical reactions, chemical reactivity with lithium metal, solubility, viscosity, and diffusion coefficients, are critically dependent on the nature of the electrolyte systems in which they are immersed.[10-13] As a result, the electrochemical properties of Li-S batteries are greatly influenced by the electrolyte system employed. Although various electrolyte systems, including ionic liquids, have been developed,[14-16] the glyme/1,3-dioxolane-based solvent systems presented by the PolyPlus battery company have been widely used due to their considerable advantages, such as high capacity, strong cycling properties, and high rate capabilities.[17,18] Recently, some additives, such as ionic liquids and $LiNO_3$, have been developed to increase the cycle performance of Li-S batteries.[11,12,19,20] It was reported that the cycle properties and coulombic efficiency were dramatically enhanced by the addition of $LiNO_3$ to liquid electrolytes.[19,20] To date, various glymes ($CH_3O(CH_2CH_2O)_nCH_3$), including 1,2-dimethoxyethane (DME, monoglyme), di(ethylene glycol) dimethyl ether (DGM, diglyme), and tetra(ethylene glycol) dimethyl ether (TGM, tetraglyme), have been studied in combination with 1,3-dioxolane (DOX), which is known to form a stable passive film on lithium metal surfaces.[21] We postulated that mixed electrolyte systems

may have an optimal composition such as that of lithium-ion batteries, which are composed of a linear carbonate and a cyclic carbonate solvent. In this work, the electrochemical performance of Li-S cells in ternary electrolyte systems containing DME, TGM, and DOX was investigated. DME (M_w = 90.1 g/mol) with a low viscosity (η = 0.455 cP at 25 °C) was chosen as a representative low-molecular-weight glyme solvent. In contrast, TGM (M_w = 222.3 g/mol) with a high viscosity (η = 4.05 cP at 25 °C), which is known to provide a high discharge capacity, was selected as a representative high-molecular-weight glyme solvent.[17] Data for the cycle performance and discharge capacities at various C rates were obtained for ten different electrolyte compositions and examined by using a statistical approach that has been frequently used to optimize products in the private sector.

Experimental

The sulfur cathodes were composed of 65 wt % elemental sulfur as an active material, 15 wt % Ketjenblack as an inert electrode, and 20 wt % polyethylene oxide (M_w = 1,000,000) as a binder. The three materials were mixed with an acetonitrile solvent by a ball-milling method to create a slurry mixture with an appropriate viscosity. Sulfur cathodes were produced by casting the mixture slurry on a carbon-coated aluminum current collector by the doctor blade method. The average loading level of sulfur was 2 mg/cm^2. The sulfur cathodes were dried at 60 °C under vacuum for more than 6 h before assembly. Lithium metal foil was used as an anode to assemble CR2016 coin cells in an argon-filled glove box. After removing water with molecular sieves, 1,2-dimethoxyethane (DME, monoglyme), tetra(ethylene glycol) dimethyl ether (TGM, tetraglyme), and 1,3-dioxolane (DOX) were used as organic solvents for the ternary electrolyte systems. The volumetric ratios of the three solvents for the ten electrolyte compositions presented in Table 1 were designed with the mixture DOE (design of experiments) tool of the Minitab program (ver. 16). Ten electrolytes with different compositions were prepared by dissolving 1 M $LiN(CF_3SO_2)_2$ (LiTFSI) and 0.1 M $LiNO_3$ in each solution. Charge/discharge tests of the Li-S cells with different electrolyte compositions were performed in the voltage range of 1.8-2.7 V versus Li/Li$^+$ at 25 °C. The discharge rates of Li-S cells were sequentially changed for the four initial cycles (0.1 C → 0.2 C → 0.5 C → 1.0 C), whereas the charge rate was fixed at 0.2 C (1.0 C = 838 mA/g-sulfur). The specific energy for the test cells was calculated based on the weight of elemental sulfur by considering the cell voltage and capacity of the discharge curves. Thereafter, practical cycle tests were performed from the fifth cycle for 40 additional cycles at a fixed charge/discharge rate of 0.5 C. In this work, the fifth cycle was defined as the first cycle of the cycle performance tests. The capacity values obtained at various C rates, specific energy, and cycle performance data at each composition were systematically handled by using statistical software (Minitab program, ver. 16) to predict the optimal composition of the ternary system.

Results and Discussion

Figure 1 shows examples of discharge curves of Li-S cells with different electrolytes containing 1.0 M $LiN(CF_3SO_2)_2$ and 0.1 M $LiNO_3$ as salts. For the four initial cycles, the discharge capacities were obtained by increasing the C rate sequentially from 0.1 C to 1.0 C. Test cells containing DME, DOX, or DME/TGM/DOX (1:1:1, v/v) showed a similar capacity greater than 1100 mAh/g and a midvoltage of ~2.1 V at the first discharge but a large difference in capacity at a rate of 1.0 C. In contrast, the test cell containing TGM showed a relatively low capacity of ~900 mAh/g and a midvoltage of ~2.0 V at the first discharge. Table 1 summarizes the results obtained for the discharge capacity and the midvoltage for the four initial cycles of the test cells with different electrolyte compositions. The discharge capacity and midvoltage were clearly dependent on the electrolyte composition. In fact, the difference in discharge capacity became

Table 1. Summary of the discharge capacities at various C rates and specific energies at 1.0 C for ten different electrolyte solutions containing 1 M $LiN(CF_3SO_2)_2$ and 0.1 M $LiNO_3$

Electrolyte Composition[a]			0.1 C		0.2 C		0.5 C		1.0 C		Specific Energy[b] (Wh/kg)
DME	TGM	DOX	Mid-V (V)	Capacity (mAh/g)	Mid-V (V)	Capacity (mAh/g)	Mid-V (V)	Capacity (mAh/g)	Mid-V (V)	Capacity (mAh/g)	
0	0	1	2.13	1120	2.12	975	2.08	845	2.03	697	1455
1	1	1	2.09	1132	2.08	974	2.04	871	2.00	751	1570
1	1	0	2.06	1040	2.05	798	2.00	652	1.96	581	1208
0	1	0	2.02	897	2.02	829	1.97	650	1.88	482	988
4	1	1	2.08	1134	2.08	991	2.06	922	2.03	824	1723
1	1	4	2.11	1142	2.11	1015	2.09	957	2.06	882	1857
1	0	1	2.11	1239	2.11	1093	2.09	1011	2.07	930	1968
0	1	1	2.09	1204	2.08	1014	2.04	815	1.97	705	1471
1	4	1	2.06	1189	2.05	965	2.01	801	1.94	643	1332
1	0	0	2.11	1121	2.11	1024	2.09	940	2.05	867	1826

[a]Volumetric ratio of the ternary systems consisting of DME, TGM, and DOX. [b]Specific energy calculated from the discharge curve obtained at 1.0 C.

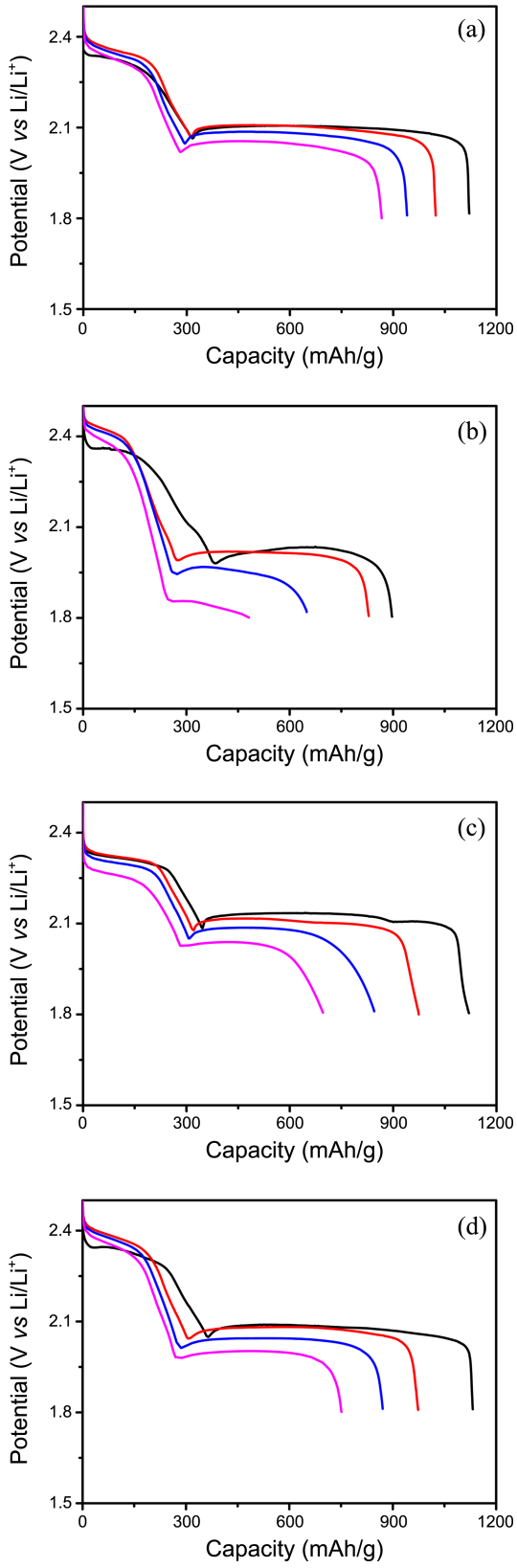

Figure 1. Discharge curves for the four initial cycles of Li-S cells with different electrolyte solutions: (a) DME/TGM/DOX (1/0/0); (b) DME/TGM/DOX (0/1/0); (c) DME/TGM/DOX (0/0/1); (d) DME/TGM/DOX (1/1/1). The discharge rates were sequentially changed for the four initial cycles: 0.1 C (—) → 0.2 C (—) → 0.5 C (—) → 1.0 C (—).

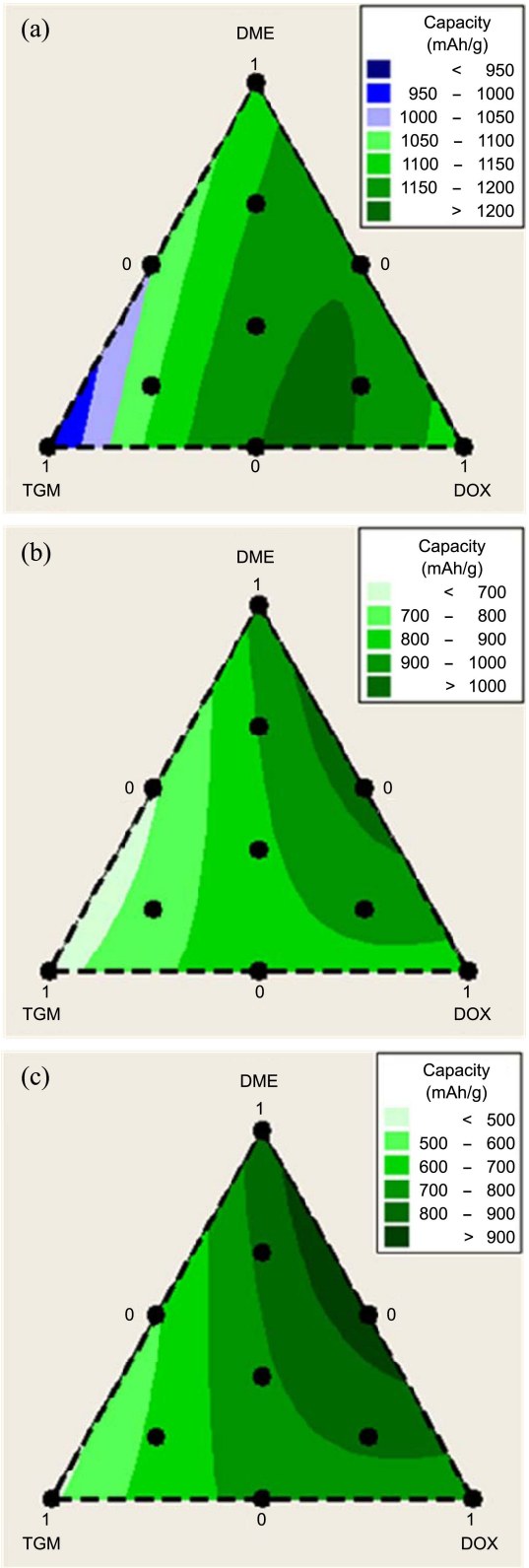

Figure 2. Mixture contour plots of discharge capacities obtained at 0.1 C (a), 0.5 C (b), and 1.0 C (c).

quite pronounced as the C rate increased. To predict the optimal composition of the ternary electrolyte, discharge capacity values at the ten electrolyte solutions were examin-

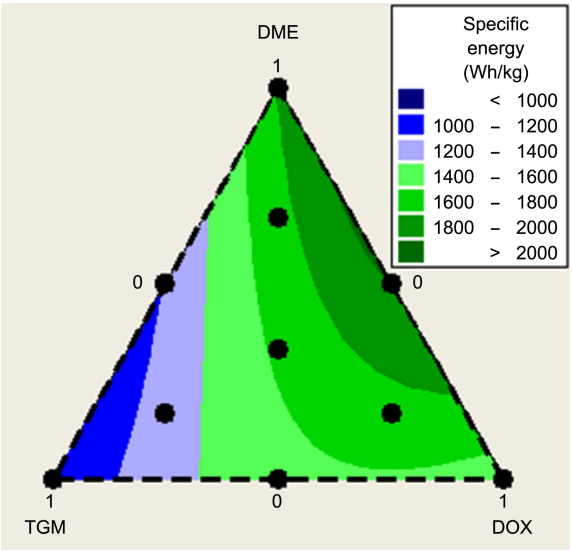

Figure 3. Mixture contour plots of specific energy calculated from the discharge curves obtained at 1.0 C.

ed by using the Minitab software. The statistical calculation led to the typical mixture contour plots shown in Figure 2. The ten filled circles in the contour plots of the ternary system indicate the electrolyte compositions used in this work. The first discharge capacities obtained at 0.1 C tended to decrease as the TGM content increased. Quite interestingly, high capacities greater than 1200 mAh/g were expected at electrolyte compositions in the following ranges: 0.0-0.4 DME; 0.1-0.5 TGM; and 0.5-0.7 DOX. This result indicates that DOX significantly contributed to not only the efficient passivation of the lithium metal anode but also to the redox reactions of sulfur and polysulfides. In contrast, the capacities at the higher C rates sharply increased with a decrease in the TGM content. Extremely high capacities greater than 900 mAh/g at a rate of 1.0 C were predicted at electrolyte compositions with a DME/TGM/DOX volume ratio of 1/0/1. However, test cells with a high TGM content showed poor rate capability properties. We believe that this feature may arise from the high solution resistance and high mass transfer overpotential due to the high viscosity of TGM

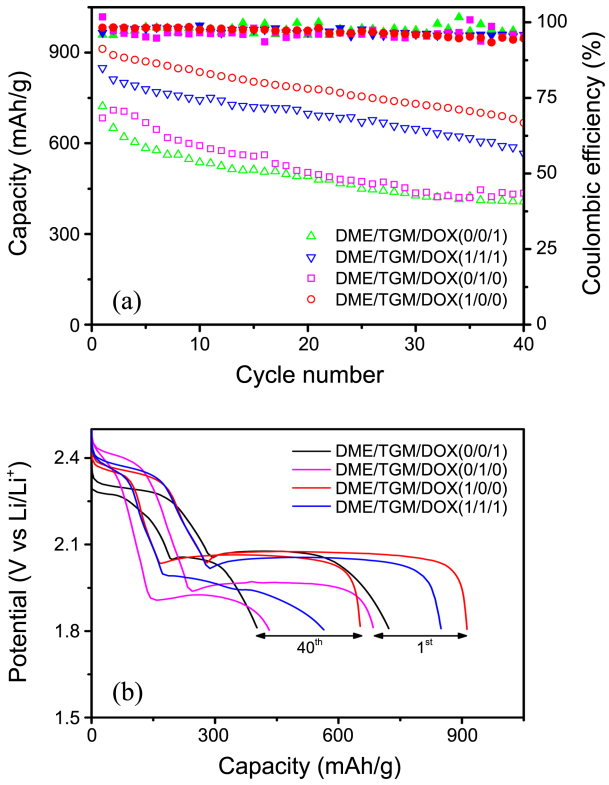

Figure 4. (a) Cycle performance of Li-S cells with different electrolyte solutions. (b) Typical discharge curves obtained at the 1st and 40th cycles.

when considering the midvoltage values and discharge profiles of the test cells (Figure 1(d) and Table 1). In fact, the discharge capacities of test cells with DME/TGM/DOX (0/1/0) increased by ~100 mAh/g when the cut-off voltage was lowered from 1.8 V to 1.5 V versus Li/Li^+.

The specific energies for the electrolyte composition calculated from the discharge curves measured at a rate of 1.0 C are listed in Table 1. The specific energy values in the ternary systems were also analyzed by a statistical method. Figure 3 shows the mixture contour plot of the specific energy at a rate of 1.0 C, which is quite similar to that of the discharge capacity at 1.0 C. The energy densities of the Li-S

Table 2. Summary of the discharge capacities with cycle number and capacity retention at the 40th cycle at each electrolyte composition

Electrolyte Composition			Capacity (mAh/g)					Capacity Retention at 40th cycle (%)
DME	TGM	DOX	1st	10th	20th	30th	40th	
0	0	1	722	537	492	427	407	56
1	1	1	827	725	680	631	551	67
1	1	0	692	644	613	576	531	77
0	1	0	684	592	504	436	435	64
4	1	1	912	825	758	706	669	73
1	1	4	924	752	688	656	633	69
1	0	1	955	839	744	720	719	75
0	1	1	774	624	582	482	367	47
1	4	1	784	691	637	596	533	68
1	0	0	915	839	783	733	670	73

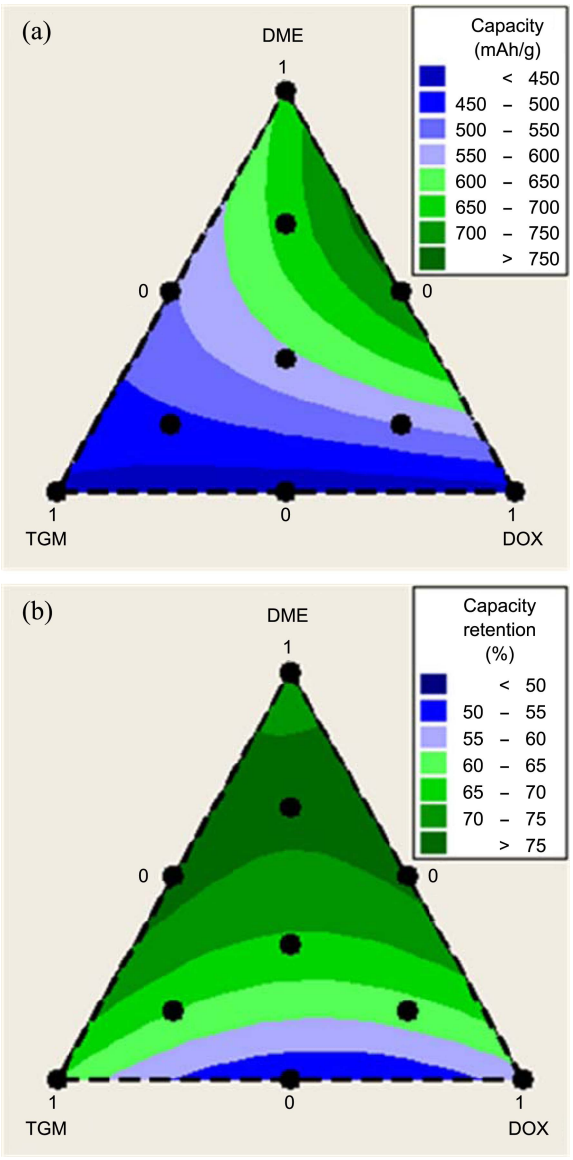

Figure 5. (a) Mixture contour plots of the discharge capacities measured at the 40th cycle. (b) Mixture contour plots of the capacity retention at the 40th cycle.

cells dramatically increased from ~1000 Wh/kg to ~2000 Wh/kg as the TGM content decreased. The test cell containing DME/TGM/DOX (1/0/1) presented the largest specific energy.

Figure 4(a) shows typical examples of the cycle performance of the Li-S cells with different electrolytes. The test cell containing DME/TGM/DOX (1/0/0) showed a relatively high capacity (670 mAh/g) and excellent capacity retention (73%) at the 40th cycle compared with those of the other three cells. On the other hand, the results showed that coulombic efficiency was not highly sensitive to the variation in electrolyte composition (Figure 4(a)). Figure 4(b) indicates that in the two plateau regions (2.2-2.4 V and ~2.0 V), the discharge capacities conspicuously decreased at the same time after 40 cycles, regardless of the type of electrolyte. Table 2 summarizes the capacity data obtained at the 1st, 10th, 20th, and 40th cycle and the capacity retention at the 40th cycle for the ten electrolytes. It is noteworthy that the test cell containing DME/TGM/DOX (0/1/1) showed the lowest capacity (367 mAh/g) and poor capacity retention (47%) at the 40th cycle. The cycle performance data for both the capacity at the 40th cycle and the capacity retention were examined with the Minitab software to obtain the mixture contour plots for the ternary system. Figure 5(a) shows that the mixture contour plot of the capacity at the 40th cycle was quite different from the plots for the initial 4 cycles (Figure 2). In general, high discharge capacities in the following ranges were predicted: 0.3-1.0 DME; 0.0-0.2 TGM; and 0.0-0.7 DOX. Figure 5(b) shows the mixture contour plot of the capacity retention at the 40th cycle. Quite surprisingly, the capacity retention, as a function of cycle number, increased significantly with the DME content in most of the compositions.

Conclusion

The discharge performance of Li-S cells was investigated for ten different electrolyte solutions containing DME, TGM, or DOX. Data regarding discharge characteristics such as capacity, specific energy, and capacity retention with cycling were analyzed statistically using the mixture DOE (design of experiment) tool of the Minitab program to obtain mixture contour plots of the discharge characteristics and to predict the optimal composition of the ternary solvent system. The statistical analysis yielded the following important results: 1) In general, the discharge capacities at a high C rate of 1.0 C were inversely proportional to the TGM content. 2) Huge capacities greater than 900 mAh/g, even at 1.0 C, were predicted for the electrolyte composition of 1/0/1 (v/v) DME/TGM/DOX. 3) The capacity retention with cycling increased significantly with the DME content. The overall results indicate that when considering the capacity in conjunction with the C rate, specific energy, and cycle properties, the optimal composition of the ternary systems is 0.5-0.8 DME; 0.0-0.1 TGM; and 0.2-0.5 DOX. The statistical approach used in this work can be extended to determine the optimal composition of various electrode materials or composite cathodes and can be applied to other mixed electrolyte systems.

Acknowledgments. This study was supported by the Research Program of the Semiconductor/Display Cluster in KOREATECH and the mid- and long-term nuclear research and development program through the National Research Foundation of Korea (NRF-2012M2A8A5025699) funded by the Korean Ministry of Science, ICT, and Future Planning.

References and Notes

1. Jeon, B. H.; Yeon, J. H.; Kim, K. M.; Chung, I. J. *J. Power Sources* **2002**, *109*, 89.
2. Jin, B.; Kim, J.-U.; Gu, H.-B. *J. Power Sources* **2003**, *117*, 148.
3. Jung, Y.; Kim, S. *Electrochem. Commun.* **2007**, *9*, 249.
4. Ji, X.; Lee, K. T.; Nazar, L. F. *Nature Mater.* **2009**, *8*, 500.

5. Levillain, E.; Gaillard, F.; Leghie, P.; Demortier, A.; Lelieur, J. P. *J. Electroanal. Chem.* **1997**, *420*, 167.
6. Gaillard, F.; Levillain, E.; Lelieur, J. P. *J. Electroanal. Chem*. **1997**, *432*, 129.
7. Levillain, E.; Gaillard, F.; Lelieur, J. P. *J. Electroanal. Chem*. **1997**, *440*, 243.
8. Han, D.-H.; Kim, B.-S.; Choi, S.-J.; Jung, Y.; Kwak, J.; Park, S.-M. *J. Electrochem. Soc*. **2004**, *151*, E283.
9. Chu, M. Y.; De Jonghe, L. C.; Visco, S. J.; Katz, B. D. *U.S. Patent* 6,030,720, 2000.
10. Kim, S.; Jung, Y.; Lim, H. S. *Electrochim. Acta* **2004**, *50*, 889.
11. Kim, S.; Jung, Y.; Park, S.-J. *J. Power Sources* **2005**, *152*, 272.
12. Kim, S.; Jung, Y.; Park, S.-J. *Electrochim. Acta* **2007**, *52*, 2116.
13. Jung, Y.; Kim, S.; Kim, B.-S.; Han, D.-H.; Park, S.-M.; Kwak, J. *Int. J. Electrochem. Sci*. **2008**, *3*, 566.
14. Yuan, L. X.; Feng, J. K.; Ai, X. P.; Cao, Y. L.; Chen, S. L.; Yang, H. X. *Electrochem. Commun.* **2006**, *8*, 610.
15. Wang, J.; Chew, S. Y.; Zhao, Z. W.; Ashraf, S.; Wexler, D.; Chen, J.; Ng, S. H.; Chou, S. L.; Liu, H. K. *Carbon* **2008**, *46*, 229.
16. Rao, M.; Song, X.; Liao, H.; Cairns, E. J. *Electrochim. Acta* **2012**, *65*, 228.
17. Choi, J.-W.; Kim, J.-K.; Cheruvally, G.; Ahn, J.-H.; Ahn, H.-J.; Kim, K.-W. *Electrochim. Acta* **2007**, *52*, 2075.
18. Wang, C.; Chen, J.-J.; Shi, Y.-N.; Zheng, M.-S.; Dong, Q.-F. *Electrochim. Acta* **2010**, *55*, 7010.
19. Liang, X.; Wen, Z.; Liu, Y.; Wu, M.; Jin, J.; Zhang, H.; Wu, X. *J. Power Sources* **2011**, *196*, 9839.
20. Zhang, S. S. *Electrochim. Acta* **2012**, *70*, 344.
21. Nimon, Y. S.; Visco, S. J.; Chu, M. Y. *U.S. Patent* 6,225,002, 2001.